Possible exotic mesons in the charmonium region

K. F. Liu and C. W. Wong
Physics Department, University of California, Los Angeles, California 90024
(Received 2 July 1979; revised manuscript received 14 February 1980)

We consider the possibility that a number of $PC = ++$ mesons might appear in the charmonium region below $\psi'(3.69$ GeV). They are states made up of admixtures of $c\bar{c}g$ (g = gluon), $c\bar{c}q\bar{q}$ ($q = u,d$), and the charmonium ^3P_J states. Masses, decay widths, and mixing matrix elements are studied with the help of the model of Horn and Mandula for $c\bar{c}g$ states and the results of Jaffe, and De Rújula and Jaffe, for $c\bar{c}q\bar{q}$ states. The presence of a $c\bar{c}$ pair suggests narrow hadronic widths if the mass is below the breakup thresholds of the $c\bar{c}q\bar{q}$ states. Their branching ratios for γ transitions and 2γ annihilations appear to be fairly small. They may have rather large spin-spin splittings. It is plausible that the lowest-mass states contain mostly $c\bar{c}g$ configurations. Although they share part of the charmonium ^3P_J γ-cascade strengths, it is likely that they are more readily produced in the hadronic decays of vector mesons in e^+e^- annihilations. We also discuss the possible appearance of similar states in the Υ region and among light mesons. We suggest in particular that strange mesons in suitable decay modes might well provide the most ready experimental access to such gluon and four-quark states.

I. INTRODUCTION

The spectroscopy of new heavy mesons is interesting partly because so many states can be understood qualitatively as simple two-body bound states of quark-antiquark ($Q\bar{Q}$) pairs of heavy quarks.[1] For example, Fig. 1 shows the mesons in the charmonium region at and below ψ' (3.69 GeV) which were known or suspected before the summer of 1979.[2-5] Five of these have been understood as charmonium states of a pair $c\bar{c}$ of charmed quarks: $\psi(3.10)$ and $\psi'(3.69)$ are the lowest two $^3S_1$ ($PC = --$) states and $\chi(3.41)$, $\chi(3.51)$, and $\chi(3.55)$ are the $^3P_{0,1,2}$ ($PC = ++$) states. Thus they give experimental support for the naive quark model of hadron structure, and they provide windows through which the dynamics of $Q\bar{Q}$ interactions might be glimpsed.

The remaining three mesons, namely $X(2.83)$, $\chi(3.45$ or $3.33)$, and $\chi(3.59$ or $3.18)$, might have been seen in the γ decay of $\psi'(3.69)$. Their suspected properties do not match those of any charmonium state.[1] They are very interesting objects if they exist, because they might provide us with another window on quark dynamics.

The existence of these mesons has not been established. Preliminary results from two new experiments[6-8] at SPEAR suggest that the situation might be even more uncertain than before. In the crystal-ball experiment,[6] a faint signal is seen in $\psi' \to \gamma X$ with a branching ratio (BR) of 0.1–0.5%. However, the mass of this X is 2.98 ± 0.02 GeV; the old $X(2.83)$ is not seen. The cascade γ decays $\psi' \to \gamma\chi \to \gamma\gamma\psi$ through $\chi(3.45)$ or $\chi(3.59)$ are not seen; the upper limits of these cascade BR's are 0.044% and 0.06%, respectively. Another preliminary report[7] of the crystal-ball experiment gave an upper limit for the γ-cascade BR B ($\psi \to X(2.83)\gamma \to \gamma\gamma\gamma$) of only 0.0027%. In the Mark II collaboration,[8] preliminary results on the cascade γ decay of ψ' have been reported. The resulting high-mass $\gamma\psi$ invariant-mass distribution shows clear peaks associated with $\chi(3.50)$ and $\chi(3.55)$, but no clear peaking is seen at $\chi(3.455)$ with BR $< 0.12\%$ or $\chi(3.415)$ with BR $= 0.08 \pm 0.08\%$. It is obvious that one should reserve judgment concerning the existence of these mesons until the final results become available.

What are the theoretical expectations concerning mesons in the charmonium region? Let us first recall the familiar observations[1] concerning charmonium states. The γ-cascade BR's via $\chi(3.59)$ or $\chi(3.45)$ are too small for them to be seen if they are the charmonium $2\,^1S_0(\eta_c')$ or $^1D_2$ states, while the BR for $\psi(3.10) \to \gamma\,^1S_0(\eta_c)$ is so large that the missing η_c should have been seen if its mass is not too close to that of ψ. This well-known situation is illustrated in Table I in which the calculated $M1$ widths or BR's are compared with the present experimental situation. Two different $c\bar{c}$ potentials, the spin-independent potential A from Ref. 9 and the spin-dependent potential C from Appendix A of this paper, are used to illustrate the model dependence of the γ cascade BR through η_c'. The BR at the predicted mass of 3.57 GeV (from Appendix A) for η_c' is 0.01% for potential C. This appears to be just beyond the reach of the latest experiments.

We now turn to other mesons which might appear in the charmonium region and might be accessible from $\psi'(3.69)$. It is useful to classify them according to whether they are or are not dominated by structures containing a $c\bar{c}$ pair. If they are, it is natural that they should appear in

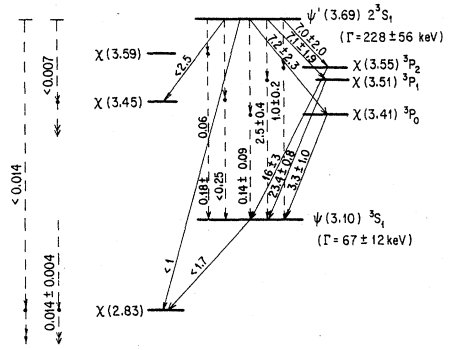

FIG. 1. Experimental situation concerning mesons in the charmonium region below $\psi'(3.69)$ before the summer of 1979. Single arrows denote single-γ transitions; double arrows denote $\gamma\gamma$ annihilations. Solid lines denote single transitions, while broken lines denote cascades for which the quoted percentages are products of branching ratios. All branching ratios are quoted as percentages. The experimental data are from Ref. 2 [for $\psi' \to \chi(^3P_J)\gamma$, $\psi' \to \chi(3.45)\gamma$, $\psi' \to X\gamma$, and $\psi \to X\gamma$], Ref. 3 (for $\psi' \to \chi\gamma \to \psi\gamma\gamma$), Ref. 4 for [for $\psi' \to (X \text{ or } \chi)\gamma \to \gamma\gamma\gamma$ and $\psi \to X\gamma \to \gamma\gamma\gamma$], and Ref. 5 (all others).

the charmonium region. Since they are not charmonium states, there should be one or more additional constituents in these structures. Relatively low masses result if both the $c\bar{c}$ and the remaining structures are separately negative-parity objects, i.e., pseudoscalars or vectors (color singlet or octet) with an S-wave relative spatial motion. Hence these mesons are likely to have $PC = ++$, and are mixed into the ^3P_J charmonium states. The presence of a $c\bar{c}$ pair also means that their annihilation widths are relatively small. Examples of these models are the $c\bar{c}g$ (g = gluon) states of Horn and Mandula,[10] and the S-wave $c\bar{c}q\bar{q}$ states (where $q = u$ or d quark) of Jaffe and De Rújula.[11,12]

It is also possible that mesons with no significant $c\bar{c}$ content will also appear in the charmonium region. Examples are the gluon bound states[13] (bound states of two or more gluons) and the multiquark states $(q\bar{q})^p$ of light quarks. The absence of significant $c\bar{c}$ content means that they do not necessarily make their first appearance in the charmonium region, so that their quantum numbers are less restricted. They are likely to be coupled relatively strongly to light-meson continua and to have relatively large hadronic widths.

Thus, mesons in the charmonium region with relatively narrow widths are likely to be states with $PC = ++$ and significant $c\bar{c}$ contents, i.e., states which can be mixed readily with the charmonium ^3P_J mesons. The possible roles of these mesons have been discussed in the literature.[10-14] In this paper, we would like to add to this discussion in a number of ways. In Sec. II, the masses of $c\bar{c}g$ states are estimated and their decay properties are discussed. Their mixing strengths into charmonium ^3P_J states are estimated. In Sec. III, the role of $c\bar{c}q\bar{q}$ states is discussed. The mixing between $c\bar{c}g$ and $c\bar{c}q\bar{q}$ states is considered in Sec. IV.

Section V contains a brief summary and concluding remarks. In particular, some of the limitations of the present qualitative discussion are pointed out. The possibility that similar structures might have been seen for lighter mesons is discussed. It is also pointed out that these mesons are perhaps more readily detectable in the hadronic decays of sufficiently massive vector mesons produced in e^+e^- annihilations.

II. $c\bar{c}g$ STATES

The $c\bar{c}g$ states have been studied by Horn and Mandula,[10] who use a representation which can be denoted by the composite spectroscopic symbol $(^3L_{J'}{}^8, {}^3l_j{}^g)J^{PC}$, where the first symbol describes the color-octet $c\bar{c}$ state and the second symbol describes the gluon state. The lowest states are $(^3S_1{}^8, {}^3s_1{}^g)J^{++}$, with $J = 0$, 1, and 2. These states are similar to, but not exactly identical with, the

TABLE I. Comparison between expected and observed $M1$ γ transition widths or branching ratios for the charmonium model of three heavy mesons. The $c\bar{c}$ potential A is from Ref. 9, while potential C is from Appendix A. The references are for the observed values.

Model	Datum	Pot. A	Pot. C	Observed	Reference
$X = {}^1S_0(\eta_c)$	$\Gamma(\psi \to X(2.98)\gamma)$ (keV)	2.8	2.7		
	$B(\psi' \to X(2.98)\gamma)$ (%)	1.3	11	0.1–0.5	6
$\chi = 2{}^1S_0(\eta_c')$	$B(\psi' \to \chi(3.59)\gamma)$ (%)	0.7	0.6		
	$B(\psi' \to \chi(3.45)\gamma)$ (%)	11	10	<0.044	6
	$B(\psi' \to \chi(3.59)\gamma \to \psi\gamma\gamma)$ (%)	4×10^{-4}	0.02	<0.06	6
	$B(\psi' \to \chi(3.45)\gamma \to \psi\gamma\gamma)$ (%)	9×10^{-4}	0.11	<0.12	8
$\chi = {}^1D_2$	$B(\psi' \to \chi(3.59)\gamma)$ (%)	0.11	0.12		
	$B(\psi' \to \chi(3.45)\gamma)$ (%)	1.8	2.1	<0.044	6
	$B(\psi' \to \chi(3.59)\gamma \to \psi\gamma\gamma)$ (%)	4×10^{-4}	5×10^{-4}	<0.06	6
	$B(\psi' \to \chi(3.45)\gamma \to \psi\gamma\gamma)$ (%)	2×10^{-3}	3×10^{-3}	<0.12	8

transverse-gluon $c\bar{c}g$ states $({}^3S_1{}^8, E1)J^{++}$, where the gluon is a transverse $E1$ radiation bound in the system.[15] This is because an Ej transverse gluon contains a fraction $(j+1)/(2j+1)$ of ${}^3(j-1)_j{}^g$ state and a fraction $j/(2j+1)$ of ${}^3(j+1)_j{}^g$ state. The Horn-Mandula representation is the more useful if the bound gluon develops an effective mass as a result of its confinement. On the other hand, the radiation states are more realistic if the bound gluons are transverse, like radiations in a cavity. In the following, we use the Horn-Mandula states for estimates of masses and matrix elements. If, in some of the qualitative discussions given below, we do not make clear which representation we might have in mind, it is because we do not know which type of state is the more realistic. This basic uncertainty of the $c\bar{c}g$ model, which arises from our ignorance of gluon dynamics, should be remembered in interpreting its results.

Horn and Mandula use the trial wave function

$$\Phi(Q\bar{Q}g)=\phi_{Q\bar{Q}}(\vec{d})\phi_g(\vec{r}) \tag{2.1}$$

to estimate the masses of the $Q\bar{Q}g$ states. For S waves, they use variational wave functions of the forms

$$\phi_{Q\bar{Q}}(\vec{d})=\frac{\mu^{3/2}}{\sqrt{8\pi}}\exp(-\tfrac{1}{2}\mu d)\,,$$
$$\phi_g(\vec{r})=\frac{\lambda^{3/2}}{\sqrt{8\pi}}\exp(-\tfrac{1}{2}\lambda r)\,, \tag{2.2}$$

where $\vec{d}$ and $\vec{r}$ are the quark (Q) and gluon coordinates, respectively, as measured from the center of mass of the $Q\bar{Q}$ pair. The Qg and $\bar{Q}g$ parts of the Hamiltonian are obtained by making an additive or universality assumption under which the gluon is dynamically equivalent to a $q\bar{q}$ pair with a strong-interaction coupling constant relevant to the masses of the $Q\bar{Q}g$ states. When allowance is made for both the linear confinement potential and the residual color Coulombic interaction, they conclude that the $c\bar{c}g$ $({}^3S_1{}^8, {}^3s_1{}^g)$ states can appear anywhere between 3 and 5 GeV.

We have repeated this variational calculation for these $c\bar{c}g$ masses using three sets of $c\bar{c}$ potentials deduced from the charmonium spectrum. (The potential A is from Ref. 9, the potential B is from Ref. 1, and the potential C is from Appendix A of this paper.) The Hamiltonian used is

$$H=\left[2m_c+p_{c\bar{c}}{}^2/m_c-\frac{1}{8}\left(2kd-\frac{4}{3}\alpha_s\frac{1}{2d}+b\right)\right]+p_g$$
$$+\frac{9}{8}\left[k(|\vec{r}-\vec{d}|+|\vec{r}+\vec{d}|)\right.$$
$$\left.-\frac{4}{3}\alpha_s\left(\frac{1}{|\vec{r}-\vec{d}|}+\frac{1}{|\vec{r}+\vec{d}|}\right)+2b\right], \tag{2.3}$$

where m_c is the c-quark mass, $p_{c\bar{c}}$ is the relative momentum of the $c\bar{c}$ pair, and p_g is the gluon momentum. The strengths k, α_s, and the additive constant b of the $c\bar{c}$ potential are given in Table II. The color factors $\frac{9}{8}$ and $-\frac{1}{8}$ give the relative strengths of Qg (or $\bar{Q}g$) in the color representation $\underline{3}$ (or $\bar{\underline{3}}$) and of the $Q\bar{Q}$ interaction in color-octet states, relative to the $Q\bar{Q}$ interaction in the color-singlet state.[10]

The calculated variational results are shown in Table II. We see that these potential models give roughly the same value of $\bar{M}\simeq 3.4$ GeV for the center of mass of the $({}^3S_1{}^8, {}^3s_1{}^g)J^{++}$ states. The rms radii of g and c (or $\bar{c}$) from the center of mass of $c\bar{c}$ are

$$r_g=\sqrt{6}/\lambda,\quad r_c=r_{\bar{c}}=\sqrt{6}/\mu\,. \tag{2.4}$$

Table II shows that the gluon ($r_g\simeq 0.2$–0.3 fm) spreads out more than the $c\bar{c}$ pair ($r_c\simeq 0.16$–0.2 fm).

These results illustrate the nature of the $c\bar{c}g$ states, but as quantitative estimates they contain many shortcomings: (i) The gluon in Eq. (2.1) is not a transverse $E1$ gluon, which contains 33% ${}^3d_1$ state. (ii) The $c\bar{c}$ wave function used is nonrelativistic. (iii) The validity and adequacy of the Hamiltonian (2.3) have not been established. (iv) The J dependence of masses is unknown.

The last item is just the hyperfine structure, which is due to a spin-spin interaction. In first-order perturbation theory, it gives an interval rule

$$R_y=\frac{Y_2-Y_1}{Y_1-Y_0}=2\,, \tag{2.5}$$

where Y_J is the mass (or name) of the $c\bar{c}g$ state of angular momentum J. Since the spin-spin interaction is known empirically to be very strong, it tends to decrease the low J state more, leading

TABLE II. Variational solutions for the $c\bar{c}g$ $({}^3S_1{}^8, {}^3s_1{}^g)$ multiplet in the Horn-Mandula model using three $c\bar{c}$ potentials fitting the charmonium spectrum.

Model	A	B	C
m_c (GeV)	1.60	1.65	1.51
k (GeV^2)	0.195	0.233	0.149
α_s	0.15	0.225	0.54
b (GeV)	−0.65	−0.75	−0.08
$\bar{M}$	3.40	3.30	3.47
λ (GeV)	1.80	2.10	2.50
μ (GeV)	2.30	2.60	3.00
$\sqrt{6}/\lambda$ (fm)	0.27	0.23	0.19
$\sqrt{6}/\mu$ (fm)	0.21	0.18	0.16
P_g (GeV)	0.76	0.89	1.06
$h(g\to q\bar{q})$ (GeV)	0.42	0.46	0.53

to a reduced interval ratio R_y. The reduction is greater when an interaction is more singular at the origin.

Before proceeding further it is necessary to estimate the mass difference $Y_2 - Y_0$ itself. A plausible model for this is to apply the Horn-Mandula additive procedure, assumed in the Hamiltonian (2.3), also to the spin-dependent part of the basic cq interaction. That is, the gluon is assumed to be dynamically equivalent to an isoscalar $q\bar{q}$ pair, where $q = u$ or d quark. It is then possible to relate $Y_2 - Y_0$ to the hyperfine mass splitting $D^* - D = 0.14$ GeV of the $D = c\bar{q}$ mesons as follows:

$$Y_2 - Y_0 \simeq \tfrac{9}{4} \times \tfrac{3}{4} (D^* - D)(r_D/r_{cg})^p . \tag{2.6}$$

Here $\frac{9}{4}$ is a color factor, $\frac{3}{4}$ is a spin factor, r_D ($\simeq r_{\rho\pi}/\sqrt{2}$, where $r_{\rho\pi}$ is an average π/ρ radius) is the average separation between c and $\bar{q}$ in the D^*/D mesons, r_{cg} [$\simeq (r_c^2 + r_g^2)^{1/2} \simeq 0.3$ fm] is the average separation between c and g in $c\bar{c}g$, and p is the power of the inverse power spin-dependent potential. The choice $p \simeq 2$ and $r_{\pi\rho} \simeq 0.6$ fm (since $r_{\pi\rho} > r_\pi = 0.56 \pm 0.04$ fm, according to Ref. 16) gives the estimate $Y_2 - Y_0 \simeq 0.5$ GeV.

Typical of the variational results obtained from the Hamiltonian (2.3) plus an additional spin-spin term of roughly this strength are the masses $Y_2 = 3.58$ GeV, $Y_1 = 3.32$ GeV, and $Y_0 = 3.00$ GeV obtained with an inverse square spin-spin potential. (For these masses, $R_Y = 0.80$ is obtained.) These results suggest that the $c\bar{c}g$ model may provide interesting mesons below $\psi'(3.69)$.

We now consider decay widths. For decays into hadrons below the charmed threshold (3.73 GeV), the leading diagrams for $J = 0$ or 2 are the two-gluon diagrams of Fig. 2, all of third order in the color charge g. Compared to $\Gamma(^3P_J \to gg)$, Fig. 2(a) carries a relative color factor of $\frac{1}{48}$, one additional power of $\alpha_s \simeq 0.2$, and a reduction factor of perhaps 10^{-1}–10^{-2} because of the additional internal quark line. Thus the hadron width from Fig. 2(a) is perhaps 10^{-4} that of $\Gamma(^3P_J \to gg)$, i.e., of the order of 0.1 keV.

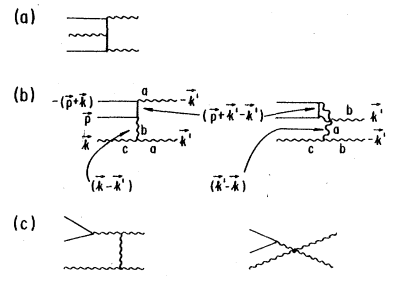

FIG. 2. Hadronic decay of $c\bar{c}g$ states.

In Fig. 2(b), the "cross" diagram cancels the direct diagram exactly under certain conditions. This cancellation can occur because unlike the usual case of $e^+e^- \to 2\gamma$, the crossed diagram carries an intrinsic negative sign because of the reversed order of the color labels in the structure constant f^{abc} at the three-gluon vertex. The extent of the cancellation depends on the particle momenta, which are also shown in Fig. 2(b). We see that between the direct and crossed diagrams, the only momentum changes are in the signs of the initial and final gluon momenta $\vec{k}$ and $\vec{k}'$. Since the initial gluon is in a state ($^3s_1{}^g$) of even spatial parity, while the final gluon also has even spatial parity, we conclude that the cancellation is exact in Fig. 2(b).

Although these QED-like diagrams suggest that the hadronic width might be small, we are unable to give even an order-of-magnitude estimate of the leading quantum-chromodynamics (QCD) diagrams shown in Fig. 2(c). This is a major shortcoming of the present discussion.

For 2γ annihilation of the $Y_{J=0,2}$ states, the analog of Fig. 2(a) is allowed, but those of Figs. 2(b) and 2(c) vanish identically if the gluon does not have an electromagnetic structure. We expect Fig. 2(a) for 2γ annihilation to be of order $\alpha_s \Gamma(^3P_{0,2} \to \gamma\gamma) \simeq 0.5$ (0.1) keV for $J = 0$ (2).

A better estimate of the 2γ annihilation width from Fig. 2(a) can perhaps be made as follows. Starting from the 3γ annihilation diagram[17] for the $c\bar{c}$ $1\,^3S_1$ state, we bend back to negative time the middle γ, and change it into a gluon. We then find that

$$\Gamma((^3S_1{}^8, E1)0^{++} \to \gamma\gamma) \simeq 3 \times 4f(\alpha_s/e_c{}^2\alpha)\Gamma(^3S_1 \to \gamma\gamma\gamma) , \tag{2.7}$$

where there is a spin-recoupling factor of 3, a color factor of 4, and a factor f to account for the reduction of phase space in the bound gluon state. Since each γ in $^3S_1 \to \gamma\gamma\gamma$ is about 1 GeV, while the bound gluon also has about the same kinetic energy, according to Table II, the factor f cannot be too small. We have not estimated it, but shall simply use the arbitrary value $f \simeq \frac{1}{2}$. Equation (2.7) is finally related to the hadronic width:

$$\Gamma((^3S_1{}^8, E1)0^{++} \to \gamma\gamma) \simeq \tfrac{216}{5} f(e_c{}^2\alpha/\alpha_s)^2 \Gamma(\psi \to \text{hadrons}) \simeq 0.4 \text{ keV} . \tag{2.8}$$

Thus the previous order-of-magnitude estimate appears to be reasonable.

Finally, we estimate the mixing strength h_J for the mixing between the $c\bar{c}g$ state and the $c\bar{c}$ ^3P_J state. If H_g (Ej) is the Hamiltonian causing the absorption of an Ej gluon, then

$$h_J(Ej) = \langle {}^3P_J \,|\, H_g(Ej) \,|\, ({}^3S_1{}^8, {}^3s_1{}^g)J\rangle$$
$$= \tfrac{2}{3}\sqrt{2}\, g\left(\frac{8}{j(j+1)}\right)^{1/2} \frac{j+1}{2j+1}(-)^j \int_0^\infty dk\, k^{j+1/2}\tilde{\phi}_g(k)\langle {}^3P_J \,||\, M_{Ej}(k) \,||\, ({}^3S_1{}^8, {}^3s_1{}^g)J\rangle/(2J+1)^{1/2}. \quad (2.9)$$

Here $\tilde{\phi}_g(k)$ is the Fourier transform of the gluon wave function in Eq. (2.2), while the reduced matrix element is that of the *nonrelativistic* operator for Ej photons (with $j=1$) shown explicitly in Appendix B. The Horn-Mandula wave function (2.1) is used for the $c\bar{c}g$ state. Since the $E1$ matrix element is not sensitive to the ${}^3P_J$ wave function, we use a spin-independent p-wave exponential wave function (with the same rms radius as the ${}^3P_{J=1}$ wave function obtained from the potential model C), so that the reduced matrix element in Eq. (2.9) can be calculated analytically.

The mixing strength h_J obtained is shown in Fig. 3 as a function of the wave-function parameters λ and μ of Eq. (2.2). We see that it depends relatively weakly on these parameters, and is of the order of 50–250 MeV. [More specifically for the state-dependent wave functions of case (a) of Sec. IV, we get $h_{J=2}=60$ MeV, $h_1=150$ MeV, and $h_0=240$ MeV.]

Now two unperturbed states separated also by h_J will mix into each other to form 72/28 mixtures separated by $2.2\,h_J$. This means that a $c\bar{c}g$ state within $2.2h_J$ of a charmonium ${}^3P_J$ state should have at least $\frac{1}{3}$ of the latter's γ-cascade BR. When the possible QCD contributions to the hadronic width of a $c\bar{c}g$ state are allowed for, the expected BR should perhaps be reduced by a factor of 2–4 to say $\frac{1}{10}$ of the ${}^3P_J$ value. This result suggests that the present experimental capability for measuring a γ-cascade BR of $\simeq 0.05\%$ makes it feasible to hunt for small splittings of the ${}^3P_{1,2}$ strengths distributed among other low-mass mesons. Eventual failure to see any such strength inside a certain mass region would mean that any $c\bar{c}g$ (or other) state which might appear inside the region is coupled to the ${}^3P_J$ state less strongly than half of the mass difference from the ${}^3P_J$ state.

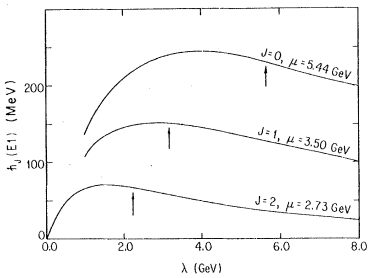

FIG. 3. The mixing strengths $h_J(E1)$ between charmonium ${}^3P_J$ and $c\bar{c}g$ states, as calculated from Eq. (2.9) with J-dependent wave functions defined in Eq. (2.2). The arrows point to the estimated values of $h_J(E1)$ using the wave-function parameters λ and μ obtained in the variational calculations described in this section and in Sec. IV. (Table IV of Sec. IV gives more details on these calculations.)

III. $c\bar{c}q\bar{q}$ STATES

The S-wave four-quark state $c\bar{c}q\bar{q}$ ($q=u,d$) have been studied by De Rújula and Jaffe.[12] When $q\bar{q}$ is in the lowest flavor quartet (similar to the pseudoscalar mesons $P=\pi,\eta$), there are two possible color-singlet combinations for $(c\bar{c})\times(q\bar{q})$: $(\underline{1}\times\underline{1})\underline{1}$ and $(\underline{8}\times\underline{8})\underline{1}$. There are six intrinsic spin states for $(\frac{1}{2})^4$: $S=(1+0)\times(1+0)=0+1+2+0+1+1$. Since $L=0$ and $J=S$, there are a total of $4\times2\times6=48$ states all with even parity. Of these states only the 12 isoscalar states are candidates for mixing with the isoscalar charmonium ${}^3P_J$ states, but we shall also discuss certain isovector states as possible models for interesting mesons.

The states in the coupling scheme given above are mixed by the antisymmetrization of quark wave functions. In the bag model where all quarks move in the same bag, it is more convenient to use the coupling scheme $(cq)\times(\bar{c}\bar{q})$. If $q=u,d$ only are considered, the flavor multiplets[11] are $\underline{\bar{3}}\times\underline{3}=\underline{9}(J=0,1,2)$, $9^*(J=0)$, $\underline{6}\times\underline{\bar{6}}=\underline{36}(J=0,1,2)$, $\underline{36}^*(J=0)$, $\underline{6}\times\underline{3}=\underline{18}$, $\underline{18}^*$, $\underline{\bar{18}}$, and $\underline{\bar{18}}^*$ (all these with $J=1$). The $\underline{9}$ and $\underline{36}$ are eigenstates of G parity with

$$G=(-)^S G_P, \text{ for } \underline{9}, \underline{9}^*, \underline{36}, \underline{36}^*, \quad (3.1)$$

where G_P is the G parity of the pseudoscalar meson P made up of $q\bar{q}$. The flavor multiplets $\underline{18}$, $\underline{\bar{18}}$ are not eigenstates of G. In diagonalizing G, two states of G parity given by Eq. (3.1) and two states with the opposite G parity are obtained. The $J=1$ states which can mix with the charmonium ${}^3P_1$ state are states of the "opposite," i.e., even, G parity. We follow Jaffe[11] by referring to these bag states collectively as C_P^c, where the superscript c refers to the presence of a $c\bar{c}$ pair. (We use the notation $c\bar{c}q\bar{q}$ to denote any four-quark state, which may or may not be a simple bag.)

The $c\bar{c}q\bar{q}$ bag states are predicted[12] to occur at and above 3.6 ± 0.1 GeV by the MIT bag model. Some of these states, of particular interest in the present discussion, are shown in Table III. The mass uncertainty is that estimated[11] for the MIT bag-model mass formula as judged by its success in fitting the masses of light S-wave hadrons.

TABLE III. Meson masses (in GeV) of four-quark meson bag states in the MIT bag model, and recoupling coefficients of these states to the "two-meson" representation. The symbols P and V denote color-singlet pseudoscalar and vector mesons, respectively; the symbols $\underline{P}$ and $\underline{V}$ denote their color-octet counterparts. $\overline{M}(\underline{V}\cdot\underline{V})$ is the center of mass of the $\underline{V}\cdot\underline{V}$ components for the 0^{++} states. The $C^c_{\pi,\eta}$ masses are from De Rújula and Jaffe (Ref. 12), while all other quantities are from Jaffe (Ref. 11). The recoupled wave functions of the $J=0$ states are the corrected results of Wong and Liu (Ref. 11). The subscript A denotes a normalized antisymmetrized product state.

J^{PG}	Flavor multiplet	C^0	C_K	$C^s_{\pi,\eta}$	$C^c_{\pi,\eta}$	PP	VV	$\underline{P}\cdot\underline{P}$	$\underline{V}\cdot\underline{V}$
0^{++}	$\underline{9}$	0.65	0.90	1.10	3.63	0.743	−0.041	−0.169	0.646
	$\underline{3\bar{6}}$	1.15	1.35	1.55	3.77	0.644	0.177	0.407	−0.623
	$\underline{\bar{9}}^*$	1.45	1.60	1.80	3.95	−0.177	0.644	0.623	0.407
	$\underline{3\bar{6}}^*$	1.80	1.95	2.10	4.13	0.041	0.743	−0.646	−0.169
	$\overline{M}(\underline{V}\cdot\underline{V})$	1.01	1.22	1.42	3.75				
2^{++}	$\underline{9}$	1.65	1.80	1.95	4.05	0	0.816	0	−0.577
	$\underline{3\bar{6}}$	1.65	1.80	1.95	4.06	0	0.577	0	0.816
						$(VP)_A$	VV	$(\underline{V}\cdot\underline{P})_A$	$\underline{V}\cdot\underline{V}$
1^{++}	$\underline{\overline{18}}$	–	1.45	1.65	3.88	0.667	0	0.236	−0.707
	$\underline{\overline{18}}^*$	–	1.80	1.95	4.06	0.236	0.707	−0.667	0

These predicted masses are all above the isovector breakup thresholds $\eta_c\pi$ expected at $\simeq 3.2$ GeV ($J=0$) and $\psi\pi = 3.25$ GeV ($J=1$) and the isoscalar threshold $\eta_c\eta$ expected at $\simeq 3.6$ GeV ($J=0$). Most of these states are also above the breakup thresholds $\psi\eta \simeq 3.7$ GeV ($J=1$), $\psi\omega \simeq 3.88$ GeV ($J=0,1,2$), $\psi\rho = 3.87$ GeV ($J=0,1,2$) and the charm threshold $D\bar{D} = 3.73$ GeV. Consequently, these mesons are expected to have large hadronic widths at these predicted masses. (The only exception[12] is an isovector 1^+ state at 3.88 GeV which has only $D\bar{D}^*$ components. It is near the threshold $D\bar{D}^* = 3.87$ GeV.) Consequently, they are not expected to be seen readily below $\psi'(3.69)$.

However, the hadronic widths are greatly reduced once the masses are moved below the lowest meson-production threshold. Thus Lipkin, Rubinstein, and Isgur[14] have suggested that $X(2.83)$ might be interpreted as the lowest $(c\bar{c}q\bar{q})0^{++}$ bag states, the isovector δ_c and the isoscalar S^*_c of the flavor multiplet $\underline{9}$, which at 0.8 GeV below the bag prediction are now safely below the lowest breakup threshold, i.e., the $\psi\pi$ and $\eta_c\eta$ thresholds, respectively. Their argument is that the equivalent $(s\bar{s}q\bar{q})0^{++}$ states predicted at 1.1 GeV, also shown in Table III, may actually appear near the $s\bar{s}$ pseudoscalar $\eta'(0.96)$ as $\delta(0.98)$ and $S^*(0.98)$. So it could also happen that δ_c and S^*_c may appear near the pseudoscalar η_c expected at $\simeq 3$ GeV.

On the other hand, while δ and S^* interpreted as the four-quark bags $C^s_{\pi,\eta}$ are only 0.1 GeV below their predicted mass, within the accuracy of the bag-model mass extrapolation procedure, a decrease of 0.8 GeV is needed for δ_c and S^*_c. This large decrease will require an explanation. It is possible (but unlikely) that the bag model is simply unreliable for such mass extrapolations. Or perhaps there are mechanisms for large mass decreases which are important only for $c\bar{c}q\bar{q}$ states. If we restrict ourselves to configuration mixing within $c\bar{c}q\bar{q}$ states, it is not easy to see how such a large mass decrease can arise. One, and perhaps the only, possibility occurs if we have a bound state of an isovector $\eta_c\pi$ pair of pseudoscalar mesons. This possibility cannot be excluded by the argument that there is no $\pi\pi$ bound state, or that the small mass difference between $\delta(0.98)$ and $S^*(0.98)$ appears to be inconsistent with their being the $\eta_s\pi$ and $\eta_s\eta$ bound states, respectively, when π and η differ so much in mass. This is because the dynamical situation is somewhat different here. For example, the pion charge radius is known experimentally to be[16] 0.56 ± 0.04 fm. Hence the $\eta_c\pi$ system looks like a nucleated pion, while $\pi\pi$, $\eta_s\pi$, and $\eta_s\eta$ are quite close to the four-quark states of Table III. It is thus possible that $\eta_c\pi$ is bound. The binding cannot be very strong, however. This is because there is no one-gluon-exchange interaction between the two color-singlet substructures. We also do not expect any significant attraction in the center of the pion where the η_c is located from one-boson-exchange mechanisms of the type responsible for nuclear forces, since these are likely to be surface or peripheral processes. The most likely mechanism is probably the configura-

tion mixing effect with $c\bar{c}q\bar{q}$ bag states. If this picture is correct, it is doubtful that the effect is strong enough to provide the 0.3–0.4 GeV of binding needed to bring the $\eta_c\pi$ mass down to the old $X(2.8)$, assuming that η_c has a mass of $\gtrsim$3.0 GeV. (Such a large mass is expected for η_c, for otherwise the $M1$ γ transition $\psi \to \eta_c\gamma$ with its large γ energy and large $M1$ γ width should have been seen experimentally.) An $\eta_c\pi$ model for the new $X(2.98)$ might be more feasible, but even here the required binding of almost 0.2 GeV might present some problem.

The decay properties of $c\bar{c}q\bar{q}$ states appear to be as follows. Let us first consider γ transitions to and from charmonium states. Such transitions also require the annihilation of the light $q\bar{q}$ pair. For a color-octet $q\bar{q}$ pair, this can be accomplished readily via a virtual gluon, but two virtual gluons are needed for a color-singlet $q\bar{q}$ pair. The photon can be emitted or absorbed by either the heavy or the light quark (or antiquark) in isoscalar four-quark states, but only by the light quark (or antiquark) in isovector states. In other words, an isoscalar state decays both through the ^3P_J admixture in these mesons and through admixtures of four-quark components in the initial or final charmonium states. Thus their γ widths are not completely negligible. In contrast, an isovector state can decay only through admixtures of four-quark components in charmonium states. For example, an $E1$ transition to or from ψ or ψ' involves those four-quark components with one light quark in an orbital p wave. Since the L-excited four-quark states have higher unperturbed masses, their admixture probabilities in ψ or ψ' are smaller than ^3P_J admixture probabilities in four-quark states. The corresponding γ width should also be smaller. The most unfavorable case is probably that of an isovector four-quark state with a color-singlet $q\bar{q}$ substructure such as the $\eta_c\pi$ bound state discussed earlier. The need for an additional virtual gluon means that its γ widths might well be smaller by two or three orders of magnitude.

The strong isospin effect is absent in 2γ annihilations, since each quark-antiquark pair annihilates via the charge-dependent electromagnetic interaction. The dominant process besides ^3P_J mixing involves the color-octet components (see Table III) of $c\bar{c}q\bar{q}$ bag states, as shown in Fig. 4(a). Compared with $\Gamma(^3P_J \to \gamma\gamma) \simeq 1$ keV, the result for Fig. 4(a) should contain the additional factors of (i) $\alpha_s^{\,2} \simeq 0.1$, (ii) a relative color factor of $\frac{2}{27}$ (the color factor is $\frac{2}{9}$ instead of 3), and (iii) a reduction factor of perhaps 10^{-1} or 10^{-2} for the additional internal lines, giving an estimate of 10^{-3}–10^{-4} keV. Furthermore, if the $c\bar{c}q\bar{q}$ state contains

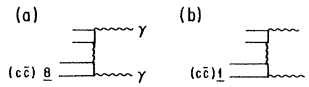

FIG. 4. Decays of $c\bar{c}q\bar{q}$ states.

two color-singlet mesonic substructures, an additional virtual gluon must be exchanged between the substructures. As a result, the 2γ annihilation width is probably $\simeq 10^{-5}$ keV only. All these annihilation widths appear far too small to be detected at present.

The hadronic width below breakup thresholds is probably not large. For isoscalar states, the dominant process besides ^3P_J mixing is that of Fig. 4(b) involving color-singlet mesonic substructures. Compared with $\Gamma(^3P_J \to gg) \simeq 1$ MeV, the relative color factor is $\frac{1}{3}$ (the actual color factor being $\frac{2}{9}$ instead of the $\frac{2}{3}$ for $^3P_J \to gg$). The presence of a virtual gluon may then bring the hadronic width down to perhaps 1 or 10 keV. Isovector states with color-octet substructures can decay via a mechanism similar to Fig. 4(b) if the virtual particle is a photon. Its width is perhaps $\lesssim$1 keV. Isovector states with color-singlet substructures can decay through ^3P_J admixtures generated by the electromagnetic interaction. The resulting hadronic widths are of the order of a few keV, but depend sensitively on the mass difference of the states before mixing. Thus hadronic widths do not appear very large. They are particularly small for isovector states.

Finally, we consider the mixing strengths $h_J(c\bar{c}q\bar{q} \to {}^3P_J)$. The leading contribution arises from the simple annihilation of a color-octet $q\bar{q}$ pair by the strong spin-flipping gluon magnetic interaction. We have not calculated these strengths, but expect it to be spin dependent and of the order of hyperfine mass splitting in charmonium, i.e., $\simeq$0.1 GeV.

In summary, we note that there are $c\bar{c}q\bar{q}$ states which could appear as weak signals in the decay of $\psi'(3.69)$ if their masses are below breakup thresholds. The trouble is that the masses predicted for these states in the MIT bag model appear too high and are probably above breakup thresholds. The only promising low-mass four-quark structure appears to be a bound $\eta_c\pi$ isovector state. Unfortunately, the γ transitions from $\psi'(3.69)$ or $\psi(3.10)$ are likely to be very weak.

IV. $c\bar{c}g + c\bar{c}q\bar{q}$ MIXING

It is clear that the component of $c\bar{c}q\bar{q}$ in which the $q\bar{q}$ pair is in a vector, color-octet state (the

$\underline{V}$ of Table III) is very similar to the $c\bar{c}g$ state. In particular, the $\underline{V}\cdot\underline{V}$ component of a $c\bar{c}q\bar{q}$ state mixes with the $c\bar{c}g$ configuration ($^3S_1{}^8, {}^3s_1{}^g$) with a mixing strength $h(g \rightarrow \underline{V})$ which can be calculated in terms of the gluon and $c\bar{c}$ wave functions. We use the $c\bar{c}g$ wave function of Eq. (2.1) and assume for simplicity that the center-of-mass wave function of the $q\bar{q}$ pair is also given by ϕ_g of Eq. (2.2), while the wave function of its relative motion is given by $2^{-3/2}\,\phi_{c\bar{c}}$ of Eq. (2.2) with the extra normalization factor arising from the change of coordinates to $\vec{r}=2\vec{d}$. The result, obtained in Appendix C, is

$$h(g \rightarrow \underline{V}) = A\mu(\mu/\lambda)^{1/2}, \tag{4.1}$$

where $A \simeq 0.16$ is a dimensionless constant, and λ and μ are the inverse size parameters in Eq. (2.2). The calculated values of $h(g \rightarrow \underline{V})$, shown in Table II, are $\simeq$0.4–0.5 GeV. When the spin dependence of λ, μ is included, these imply that $h_{J=2}(g \rightarrow \underline{V}) \simeq 0.4$ GeV for the $J=2$ state. We shall use this estimate in the calculations of this section. (An additional factor of $i=(-)^{1/2}$ in the matrix element of the pair-production vertex has been removed by redefining the phase of the wave function of one of the states.)

This mixing strength is distributed among the various $c\bar{c}q\bar{q}$ states shown in Table III; the off-diagonal element of the mass matrix is just the product of $h(g \rightarrow \underline{V})$ and $1/\sqrt{2}$ of the corresponding recoupling coefficients (for $J=0$ or 2) of the $\underline{V}\cdot\underline{V}$ component of $c\bar{c}q\bar{q}$ states shown in Table III. (The factor $1/\sqrt{2}$ arises from the antisymmetrization of the $c\bar{c}q\bar{q}$ wave function because of which only half of the $\underline{V}\cdot\underline{V}$ probability is in the "flavor decay channel"[11] $\underline{\psi}\cdot\underline{\rho}$, while the missing half is in the $\underline{D}^*\cdot\underline{D}^*$ channel.) For $J=1$, the recoupling coefficients already contain a factor $1/\sqrt{2}$ as a result of the projection of G parity. (The missing half in the $\underline{D}^*\cdot\underline{D}^*$ channel has the opposite G parity.) Thus, the effective mixing strength is $h/\sqrt{2}$ for all J. We see also from Table III that for $J=2$ this effective mixing strength may be concentrated in one single $c\bar{c}q\bar{q}$ state at 4.06 GeV. For the four $J=0$ $c\bar{c}q\bar{q}$ states, the calculation is done by diagonalizing 5×5 matrices.

Our interest in the mixing problem is twofold. First, we notice that when a strong spin-spin potential between the gluon and the quarks is added to the $c\bar{c}g$ Hamiltonian (2.3), the variational wave function (2.2) shrinks significantly as J decreases. Table IV shows two interesting examples of this J-dependent effect in the $c\bar{c}g$ wave function. Since the mixing strength h_J of Eq. (4.1) is size-dependent, $h_{J=0}$ becomes larger than $h_{J=2}$, being about twice as large in these examples. As a result, the mass ratio $(M_2-M_1)/(M_1-M_0)$ is further decreased after configuration mixing. This effect is included in the following calculation.

Second, we are primarily interested in the nature [e.g., the $c\bar{c}g$ probability $p(c\bar{c}g)$] of our mixed states. The answer is unfortunately very sensitive to the mass difference between the two types of states being mixed. It is quite plausible that the dynamical content of the $c\bar{c}q\bar{q}$ model of Sec. III is more reliable than that of the $c\bar{c}g$ model of Sec. II. We therefore decided to readjust the average mass $\overline{M}$ of the $c\bar{c}g$ states and study the dependence of $p(c\bar{c}g)$ on the mass of the lowest J^{++} state after mixing.

Figure 5 shows the results obtained for a spin-spin gluon-quark interaction of the form

$$H_{ss} = V_{ss}\sum_{i=q,\bar{q}}(\vec{\lambda}_i\cdot\vec{\Gamma}_g)(\vec{s}_i\cdot\vec{S}_g)\frac{1}{|\vec{r}-\vec{r}_i|^2}, \tag{4.2}$$

where $\vec{\lambda}$, $\vec{\Gamma}$ are color-SU(3) operators and $\vec{s}$, $\vec{S}$ are spin operators. Figure 5(a), showing the spin-spin splittings as a function of V_{ss}, is obtained with a

TABLE IV. Details of two J-dependent solutions of the $c\bar{c}g$ and $c\bar{c}q\bar{q}$ mixing problem described in Sec. IV. Here M_J is the meson mass, λ_J and μ_J are the wave-function parameters of Eq. (3.2), and $p(X)$ is the percentage of the configuration X in the wave function. Different values of the center of mass $\overline{M}(c\bar{c}g)$ have been used in these cases in order to have the final mass $M_{J=0}$ appear at 2.83 GeV.

Case		a			b	
V_{ss} (GeV^{-1})		−1.83			−1.96	
$\overline{M}$ (GeV)		3.48			3.65	
	$J=2$	$J=1$	$J=0$	$J=2$	$J=1$	$J=0$
M_J (GeV)	3.45	3.18	(2.83)	3.59	3.30	(2.83)
λ_J (GeV)	2.22	3.15	5.45	2.20	3.22	6.80
μ_J (GeV)	2.73	3.49	5.30	2.71	3.54	6.32
p $(c\bar{c}g)$	0.82	0.81	0.77	0.73	0.74	0.71
p $(\underline{V}\cdot\underline{V})$	0.20	0.10	0.20	0.08	0.12	0.26

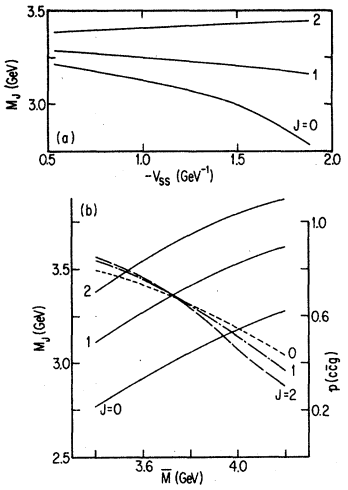

FIG. 5. (a) Mass M_J (GeV) of the lightest meson of angular momentum J obtained in the $c\bar{c}g + c\bar{c}q\bar{q}$ configuration mixing calculation described in the text, plotted as a function of the assumed strength V_{ss} (in GeV^{-1}) of the spin-spin interaction in Eq. (4.2). A center of mass $\overline{M}(c\bar{c}g) = 3.474$ GeV is used. (b) Mass M_J and $c\bar{c}g$ probability $p(c\bar{c}g)$ of the lightest meson of angular momentum J plotted as a function of $\overline{M}(c\bar{c}g)$. A spin-spin strength of $V_{ss} = -1.83$ GeV is used.

constant $\overline{M}(c\bar{c}g) = 3.474$ GeV, while Fig. 5(b), showing the dependence of the lowest M_J and the associated mixing probability $p(c\bar{c}g)$ on $\overline{M}$, is obtained with a constant $V_{ss} = -1.84$ GeV^{-1}. These results show that it is quite plausible to have states appear below $\psi'(3.69)$ which are predominantly $c\bar{c}g$ states. Furthermore, their $c\bar{c}g$ contents increase rapidly as their masses decrease below 4 GeV.

V. SUMMARY, DISCUSSIONS, AND CONCLUSIONS

In this paper we have argued that a number of $PC = ++$ mesons containing a $c\bar{c}$ substructure may appear in the charmonium region. They are states made up of admixtures of $c\bar{c}g$, $c\bar{c}q\bar{q}$, and the charmonium ^3P_J states. Their spin-spin splittings may be rather large, their hadronic widths could be fairly small if they are below the appropriate breakup threshold for the $c\bar{c}q\bar{q}$ states, their BR for γ transitions and for 2γ annihilations appear to be fairly small.

We have discussed the masses, widths, and mixing of these states. Our estimates should not be taken as firm predictions because of a number of theoretical uncertainties. They arise because of our ignorance of quark-gluon dynamics, of relativistic effects in wave functions and operators, and of the nature of the gluon in $c\bar{c}g$ states. In addition, unusual QCD contributions to the hadronic widths have not been included in our discussion.

TABLE V. Expected center of mass $\overline{M}$ of $Q\bar{Q}g$ ($^3S_1{}^8$, $^3S_1{}^g)J^{++}$ states. All quantities are in Gev, except k (GeV^2), α_s (dimensionless), and r_Q (dimensionless).

Structure	$u\bar{u}g$		$s\bar{s}g$	$c\bar{c}g$	$b\bar{b}g$
m_Q	0.16	0.12	0.33	1.51	4.8
k	0.092	0.080	0.101	0.149	0.205
α_s	1.2	1.4	0.88	0.54	0.40
b	−0.17	−0.08	−0.08	−0.08	−0.08
λ	1.98	1.94	2.00	2.53	2.86
μ	1.34	1.21	1.66	2.97	4.45
$M_{Q\bar{Q}}$	1.06	1.04	1.21	3.43	9.97
p_g	0.84	0.82	0.85	1.07	1.21
V_g	−1.59	−1.59	−1.12	−1.03	−0.96
$\overline{M}(Q\bar{Q}g)$	0.30	0.27	0.88	3.47	10.21
$M(^3S_1)$	0.783	0.783	1.020	3.10	9.46
r_Q	0.34	0.30	0.47	1.00	1.73

From the broader perspective of meson spectra in general, it is clear that if these mesons appear in the charmonium region, other $Q\bar{Q}g$ states should also appear with masses near those of $Q\bar{Q}$ mesons. Using the model of Sec. II with the spin-independent Hamiltonian (2.3) and the potential parameters of certain *spin-dependent* nonrelativistic $Q\bar{Q}$ potentials that we have fitted, in Appendix A, to the spectra of known $Q\bar{Q}$ mesons, we find the results of Table V for the masses of $Q\bar{Q}g$ states. The quantities tabulated have been defined earlier in Eqs. (2.2) and (2.3), except for the mass $M_{Q\bar{Q}}$ of the $Q\bar{Q}$ substructures in $Q\bar{Q}g$ and the potential energy V_g between g and $Q\bar{Q}$. (The gluon kinetic energy is p_g.) The masses $M_{Q\bar{Q}}$, p_g, and V_g are the expectation values of the three groups of terms shown in the $Q\bar{Q}g$ Hamiltonian (2.3). The observed mass $M(^3S_1)$ of the $Q\bar{Q}$ vector meson is also shown for comparison. We see that $M_{Q\bar{Q}}$ for the substructure $^3S_1{}^8$ is on the average about 0.3 GeV above $M(^3S_1)$, with the mass difference increasing as the quark mass m_Q increases. It is the bound gluon, however, which controls the behavior of $\overline{M}(Q\bar{Q}g) - M(^3S_1)$. Its contribution is large and negative for small m_Q, roughly zero in $c\bar{c}g$, and repulsive in $b\bar{b}g$. The reason for this behavior is that with the decrease in size of the $Q\bar{Q}$ substructure as m_Q increases, the gluon wave function is also pulled in, so that its kinetic energy increases. At the same time, the strong coupling constant α_s decreases as required by the idea of asymptotic freedom,[18] so that the magnitude of the attractive gluon interaction decreases. These two effects combine to give the strong trend seen in Table V. This behavior is thus a simple consequence of the assumed dynamics of our $Q\bar{Q}g$ model.

There is, in addition, a spin-spin splitting. We recall that the strength of the spin-spin term of the Breit-Fermi $Q\bar{Q}$ interaction is proportional to m_Q^{-2}. Since we have only one Q in the gQ interaction, we assume a m_Q^{-1} dependence, and obtain the following estimate for the mass difference between $J=2$ and $J=0$ states:

$$(M_2 - M_0)_Q \simeq \frac{m_c}{m_Q}(\lambda_Q/\lambda_c)^2(M_2 - M_0)_c . \tag{5.1}$$

Using $(M_2 - M_0)_c \simeq 0.7$ GeV, we get $(M_2 - M_0)_b \simeq 0.3$ GeV.

It is also clear that there are $Q\bar{Q}q\bar{q}$ states as well. From Tables III and V, we estimate that the 0^{++} $b\bar{b}q\bar{q}$ states $C^b_{\pi,\eta}$ might first appear at 10.2 GeV, with their weighted center of mass $\overline{M}(\underline{V}\cdot\underline{V})$ at $\simeq$10.3 GeV. The mixing strength $[h_2(q \rightarrow \underline{V})]_b$ with the $b\bar{b}g$ 0^{++} state will be stronger than $(h_2)_c \simeq 0.4$ GeV by a factor

$$r_Q = \frac{\mu_Q}{\mu_c}\left(\frac{\mu_Q/\lambda_Q}{\mu_c/\lambda_c}\right)^{1/2} \tag{5.2}$$

[where μ and λ are the inverse length parameters of Eq. (2.2)]. This factor is also tabulated in Table V. Next we estimate $(h_0)_b/(h_2)_b \simeq 1.35$ when $(M_2 - M_0)_b \simeq 0.3$ GeV. Putting everything together with configuration mixing, as described in Sec. IV, we find that there might be a 0^{++} X_b (9.34) in the Υ region just below Υ (9.46). Similar $b\bar{b}g + b\bar{b}q\bar{q}$ mixing calculations can be made for $J=1$ (2). Starting from an estimated four-quark bag mass of 10.34 (10.43) GeV, we obtain $M_J = 9.56$ (9.73) GeV for the lightest state of $J^{PC} = 1^{++}$ (2^{++}). In these mixed states, the percentage probability of the $c\bar{c}g$ component is found to be 60 (58, 56)% for $J=0$ (1,2).

The results of Table V for light mesons are obviously unsatisfactory, even without including the very considerable spin-spin mass splittings expected here. It is likely that the model wave function Eq. (2.2) is just too crude for these light mesons. It is certainly true that the interactions are stronger here, so that the many uncertainties in our knowledge of gluon dynamics are magnified. Uncertainties in this mass region also appear more serious simply because the actual meson masses are small. More detailed studies will be needed to determine the extent to which the unsatisfactory results might be related to defects in our models, or to our choice of potential parameters. (For example, the gluon should perhaps be be in an $E1$ mode.) One result of the calculation should be trustworthy: The size of a $Q\bar{Q}g$ meson increases as its mass decreases. As a consequence, the mixing strength $h_{J=0}$ between $Q\bar{Q}g$ and four-quark states should be weaker. In addition, configuration-mixing effects are reduced by the larger mass differences seen or expected in this mass region. It is then plausible that an X might coexist with a low-lying four-quark bag C^0 under a broad structure at $\epsilon(0.7)$. The interpretation of $\epsilon(0.7)$ as a four-quark state has been given recently by Holmgren and Pennington.[19]

Both the experimental situation and the theoretical picture for low-mass scalar mesons appear rather obscure. The situation is not completely hopeless, however, since mesons of the K^* family, by virtue of their strangeness, are likely to be more readily identified and analyzed. Of the eleven mesons of the K^* family tabulated by Leith,[20] two are scalars. The remaining nine mesons can be understood in terms of the simple $Q\bar{Q}$ picture. In Appendix A, a simple nonrelativistic but spin-dependent $Q\bar{Q}$ potential model is constructed globally for these mesons and mesons of other families. This model gives for the K^* family a scalar $^3P_0$ state at 1.2 GeV, where there is an observed scalar $\kappa(1.2)$ with a very broad width $\Gamma \simeq 0.45$ GeV. We interpret this width as an indication that it contains also our gluon state X_K, e.g., $u\bar{s}g$ ($^3S_1{}^8$, $^3S_1{}^g$)0^{++}, as well as the lowest four-quark scalar $C_K(\underline{9})$. The latter has been predicted by Jaffe[11] at 0.9 GeV, as shown in Table IV. We then interpret the second observed scalar $\kappa'(1.43)$, with width 0.25 GeV, as Jaffe's $C_K(\underline{36})$ which is expected at 1.36 GeV. The axial vectors $C_K(\underline{\overline{18}})1^{+\pm}$ predicted at 1.45 GeV might well be part of the broad ($\Gamma \gtrsim 0.25$ GeV) $Q_A(1.34)$ and the narrower ($\Gamma \gtrsim 0.11$ GeV) $Q_B(1.36)$, respectively. Both are known[20] to decay by $K^*\pi$ and $K\rho$ modes predicted by Jaffe's model. It would be useful to look experimentally for the remaining C_K bag states—$C_K(\underline{9}^*)$ in the $K\pi$ or $K^*\rho$ decay mode, $C_K(\underline{36}^*)0^{++}$ and $C_K(\underline{9}$ or $\underline{36})2^{++}$ in the $K^*\rho$ decay mode. The possibility of making more definite identification of these bag states by using observed branching ratios into two distinct decay modes, as suggested by Table III, should also be pointed out.

Similar analyses for mesons of the ρ, ω, and ϕ families (with details given in Appendix A) suggest that the simple $Q\bar{Q}$ $^3P_0$ states are $\delta(0.98)$ $I=1$, $S^*(0.98)$ $I=0$, and part of $\epsilon(1.3)$ $I=0$, respectively. (See Refs. 13 and 21 for the alternative interpretation of δ and S^* as four-quark states. We assume here that their $K\bar{K}$ decays are due to minority admixtures of $C^s_{\pi,\eta}$ in the wave function.) It is not clear where $s\bar{s}g$ should be, but if $u\bar{u}g$ really appears at $\epsilon(0.7)$, then $s\bar{s}g$ should also appear $\simeq$0.4 GeV higher than expected, namely at $\epsilon(1.3)$. In this mass region, one C^s_η and a number of C^0 are also expected. The large experimental width (0.2–0.4 GeV) of $\epsilon(1.3)$ appears to be consistent with this possibility. The broad ($\Gamma \simeq 0.3$ GeV) $I=1$ axial vector A_1 (~1.1) may well contain Jaffe's $C_\pi(\underline{18})1^{++}$ predicted at 1.25 GeV. This

meson does not have an isoscalar partner; the narrowness ($\Gamma \simeq 0.025$ GeV) of the $I=0$ axial vector $D(1.282)$ appears to be consistent with this picture. There are no other well-known, broad, low-lying (below the $2\,^3S_1$ state), even-parity mesons.

We have kept to the very last a discussion on the experimental production and detection of these even-P, even-C, low-lying gluon and multiquark mesons. They are of course accessible in the γ cascade decays of vector mesons if they share appreciable fractions of the $Q\bar{Q}$ ^3P_J strengths. However, the hadronic decays of sufficiently massive vector mesons

$$n^3S_1 \to A + X(J^{PC}(I^G))$$

are perhaps more promising for the production of the interesting mesons X. Table VI describes a number of light mesonic groups A associated with the production of some of the mesons which are expected, but not yet seen.

Once these mesons are observed and their quantum numbers are deduced, their place in the scheme of things can perhaps be deduced indirectly, especially when some information is also available on their decay widths. Direct evidence on the nature of these mesons probably requires at least a good knowledge of their decay modes. This requirement will not be easy to meet if we remember that the nature of the known light mesonic resonances of large widths is not yet established. For example, it is not clear from Ref. 19 if $\epsilon(0.7)$ cannot be a $q\bar{q}g$ state.

The general interpretation of meson spectra given above may be summarized by the statement that in mesons the $Q\bar{Q}$ states are most readily seen. Next come the $Q\bar{Q}g$ and four-quark states.

In conclusion, we note that the interpretation of meson spectra sketched above is necessarily very speculative and incomplete. In spite of this, our studies do suggest that significant progress can be expected when more is known about these additional low-mass mesons of the ψ, Υ, and also K^* families. Of these families, the K^* family is perhaps the most promising because of its accessibility.

TABLE VI. Some mesonic groups A associated with the production of $X[J^{PC}(I^G)]$ in the hadronic decays of vector mesons: $n\,^3S_1 \to A + X$. The symbols S or P denote the orbital angular momentum of A.

$J^{PC}(I^G)$	A	Most interesting mesons
$J^{++}(0^+)$	$S(\omega)$, $P(\pi\rho)$	$c\bar{c}q\bar{q}$, $c\bar{c}g$
$J^{++}(1^-)$	$S(\rho)$, $P(\pi\pi)$	$c\bar{c}q\bar{q}$
$J^{-+}(0^+)$	$P(\omega)$, $S(\pi\rho)$	$^1S_0$, $^1D_2$
$1^{+-}(0^-)$	$S(\eta)$, $S(3\pi)$	$^1P_1$

Note added in proof. The calculated rms radius of the K meson (0.46 fm) shown in Table VII agrees with a preliminary experimental result (from negative-kaon scattering off atomic electrons) of 0.51 ± 0.07 fm reported by E. Tsyganov, in *Proceedings of the 19th International Conference on High Energy Physics, Tokyo, 1978,* edited by S. Homma *et al.* (Physical Society of Japan, Tokyo, 1979), p. 315. See also A. Beretvas *et al.*, Report No. E1-12357, Dubna, 1979 (unpublished).

ACKNOWLEDGMENT

This work was supported in part by the National Science Foundation.

APPENDIX A: PHENOMENOLOGICAL POTENTIALS FOR $Q\bar{Q}$ MESONS

We reproduce here certain spin-dependent nonrelativistic (NR) potentials which have been used in estimating certain results mentioned in the text on γ decay widths and in providing a general perspective on $Q\bar{Q}$ states in meson spectra. These potentials are qualitatively similar to other $Q\bar{Q}$ potentials which have been reported in the literature,[22] except as noted below.

We start by fitting the excitation spectra of ρ and charmonium families of $Q\bar{Q}$ mesons independently with the NR potential models

$$H_{Q\bar{Q}} = \frac{p^2}{2\mu} + kr - \tfrac{4}{3}\alpha_s\left(\frac{1}{r} + \frac{1}{m_1 m_2} f_{BF}(r)\right) + b\,. \quad \text{(A1)}$$

Here μ is the reduced mass, b is an additive constant, and $f_{BF}(r)$ is a modified Breit-Fermi function of the form

$$f_{BF}(r) = S(r)\vec{S}_1\cdot\vec{S}_2 + W(r)\vec{L}\cdot\vec{S} + V_T(r)\vec{S}_{12}\,, \quad \text{(A2)}$$

where

$$S(r) = -\frac{2}{3}\left(\frac{4}{\pi^{1/2}r_0^{\,3}}\exp[-(r/r_0)^2]\right),$$
$$W(r) = -\tfrac{3}{2}\{1-\exp[-(r/a_0)^2]\}/r^3\,, \quad \text{(A3)}$$
$$V_T(r) = -\tfrac{1}{4}\{1-\exp[-(r/a_0)^2]\}/r^3\,,$$

and

$$\vec{S}_{12} = 3\vec{\sigma}_1\cdot\hat{r}\vec{\sigma}_2\cdot\hat{r} - \vec{\sigma}_1\cdot\vec{\sigma}_2\,. \quad \text{(A4)}$$

We have dropped the velocity-dependent Darwin term since this term is hard to treat in the three-quark problem in hadrons. We also drop the spin-independent δ-function repulsions from the spin-spin interaction. Because of these and of the intrinsic uncertainties of the NR potential model, the wave functions near the origin appear to be of questionable validity. For these reasons, we do not try to fit leptonic widths. The potentials also do not contain any isospin-dependent terms.

We do not interpret the NR potentials for the lighter mesons in a literal manner, but simply consider them as prescriptions for mass extra-

polatons. Even so, one wonders about the meaning of the mass of light quarks such as u or d in such a model. To study this question, we obtain two $u\bar{u}$ (or $d\bar{d}$) potentials, with (a) $m_u = 0.16$ GeV and (b) $m_u = 0.12$ GeV, respectively, and other parameters as shown in Table VII. The resulting $Q\bar{Q}$ meson masses are shown in Table VIII. We see that, except for the pion mass, the mass extrapolation is quite insensitive to m_u. What are changed are the rms meson radii r_M (i.e., the mean quark separations), as shown in Table VII. The experimental result[16] of $r_\pi = 0.56 \pm 0.04$ fm favors case (b).

This is good because the mass $m_u = 0.12$ GeV in case (b) is actually chosen[23] to fit the proton charge radius $r_p(D) = 0.81 \pm 0.03$ fm of the Dirac form factor F_1. [This is related to the experimental[24] charge radius $r_p(E) = 0.88 \pm 0.03$ fm of the electric form factor G_E as follows:

$$r_p^2(D) = r_p^2(E) - \frac{3}{2M_p^2}\kappa_p , \tag{A5}$$

where $\kappa_p = 1.79$ is the proton anomalous moment, and M_p is the proton mass.] The calculation of the properties of protons and other baryons was made by Rondinone and Wong[23] with the following partial results for these two potentials:

(a) $r_p = 0.68$ fm, $\Delta - N = 0.30$ GeV, $N^* - N = 0.77$ GeV,

(b) $r_p = 0.81$ fm, $\Delta - N = 0.29$ GeV, $N^* - N = 0.76$ GeV, (A6)

where N^* is the first radial excitation of the nucleon N.

Thus the NR potential model for hadrons as light as pion and proton has the useful feature that the same potential can be used to describe hadron sizes. [It is also amusing to note that the calculated ρ-meson radius $r_\rho = 0.72$ fm for the preferred case (b) of Eq. (A6) confirms an earlier rough estimate[25] made in connection with the fitting of hadron mass formulas.] We use $m_u = 0.12$ GeV in all the other potentials of Table VII.

The results of Eq. (A6) also show that, as in the case for mesons, mass extrapolations for baryons using these NR potentials appear to be quite insensitive to the choice of m_u. Thus the quark masses of our model are related to hadron sizes.

The next set of potential parameters, those for the ψ/J family, are obtained independently by fitting the charmonium spectrum, with only one constraint, namely that the additive constant be fixed at $b = -0.08$ GeV. This is the $c\bar{c}$ potential called potential C in the text. We note the interesting result that for both case (b) of the $u\bar{u}$ potential and the $c\bar{c}$ potential, the cutoff parameters a_0 and r_0 of Eq. (A3) are proportional to each other:

$$(a_0/r_0)_\psi = (a_0/r_0)_\rho = 2.7 . \tag{A7}$$

We therefore use the same proportionality constant for all the other families of mesons.

We also note that our coupling constants α_s tend to be 2–3 times stronger than those of most other potentials in the literature.[22] This is of no great significance in the present context, since many $Q\bar{Q}$ meson properties depend only on certain combinations of α_s and k, our k values being significantly weaker than usual. Indeed, $c\bar{c}$ potentials with very different parameters also give roughly the same mass for the $c\bar{c}g$ state, as shown in Table III, but sizes differ significantly. Thus there are meson properties such as the relative sizes of mesons of the same family which might be different for different potentials. Our potential will provide a useful alternative for the study of such properties.

The interaction strengths α_s are expected to

TABLE VII. Potential parameters and the vector and pseudoscalar meson radii r_V and r_P for various meson families. The empirically adjusted quantities are underlined. The additive constant b used is -0.17 GeV for case (a), and -0.08 GeV for all the other potentials. The t-quark mass, given in parentheses, is the predicted value from Ref. 29.

Family	Case	m_Q (GeV)	α_s	k (GeV^2)	r_0 (fm)	a_0 (fm)	r_V (fm)	r_P (fm)
ρ/ω	(a)	0.16	1.2	0.0919	0.70	2.09	0.63	0.43
	(b)	0.12	1.4	0.0795	1.05	2.84	0.72	0.53
ψ/J		1.51	0.54	0.1492	0.083	0.224	0.21	0.15
K^*			1.14	0.0864	0.73	1.97	0.60	0.46
Υ		4.83	0.40	0.205	0.021	0.056	0.11	0.08
ϕ		0.334	0.88	0.101	0.41	1.10	0.45	0.33
D^*			1.00	0.090	0.55	1.50	0.52	0.48
F^*			0.73	0.113	0.24	0.65	0.35	0.29
D_b^*			0.97	0.090	0.52	1.39	0.51	0.49
F_b^*			0.69	0.116	0.20	0.54	0.32	0.30
G^*			0.48	0.167	0.050	0.136	0.16	0.13
T^*		(14.00)	0.32	0.278	0.0050	0.013	0.053	0.039

TABLE VIII. Comparison between observed meson masses (in GeV) and masses calculated from the nonrelativistic potential model described in Appendix A. Masses of $t\bar{t}$ mesons are expressed as mass differences (underlined in the table) from the mass of the lightest vector meson T^* of the family.

	1^3S_1	1^1S_0	$^3P_0$	$^1P_1$	$^3P_1$	$^3P_2$	2^1S_0	$^3D_1$	2^3S_1	$^1D_2$	$^3D_3$	$^3F_2$	$^3F_4$	3^1S_0	2^3D_1	3^3S_1	4^3S_1
	ρ	π	δ	B	A_1	A_2			ρ'	A_3	g		A_4				
Expt	0.776	0.14	0.980	1.231	~1.1	1.312			~1.6	1.64	1.688		1.90				
	ω	η	S^*		D?	F					ω		h				
Expt	0.783	0.549	0.980		1.282	1.271					1.668		2.040				
Th (a)	0.77	0.13	0.97		1.17	1.30		1.39	1.49		1.69						
(b)	0.77	0.24	0.98	1.07	1.18	1.32	1.32	1.39	1.49	1.56	1.71	1.73	2.04	1.95	1.99	2.07	2.57
	K^*	K	κ	Q_B	Q_A	K^{**}	K'		$K^{*\prime}$	L'?	K^{***}						
Expt	0.892	0.494	~1.2	1.36	1.34	1.435	1.450		1.65	1.765	1.780						
Th	0.90	0.55	1.19	1.28	1.32	1.41	1.47	1.57	1.60	1.69	1.77	1.90	2.08	2.05	2.11	2.13	2.60
	ϕ	η'	ϵ?		E?	f'?											
Expt	1.020	0.958	~1.3		1.416	1.516											
Th	1.02	0.65	1.27	1.40	1.40	1.50	1.53	1.64	1.67	1.76	1.82	1.95	2.10	2.06	2.13	2.15	2.60
	ψ/J	η_c	χ		χ	χ		ψ	ψ'							ψ''	ψ'''
Expt	3.097		3.413		3.508	3.554		3.772	3.686						4.159	4.040	4.417
Th	3.10	2.83	3.41	3.52	3.50	3.55	3.57	3.76	3.69	3.81	3.83	4.01	4.05	4.01	4.14	4.09	4.44
	D^*	D															
Expt	2.006	1.863															
Th	2.01	1.90	2.42	2.46	2.46	2.49	2.65	2.77	2.69	2.81	2.83	3.07	3.13	3.18	3.26	3.21	3.66
	F^*	F															
Expt	2.14	2.03															
Th	2.09	1.92	2.43	2.51	2.50	2.55	2.64	2.78	2.72	2.83	2.85	3.05	3.11	3.11	3.21	3.17	3.57
	Υ								Υ'							Υ''	
Expt	9.46								10.03							10.43	
Th	9.46	9.19	9.89	9.95	9.94	9.97	9.98	10.21	10.07	10.22	10.23	10.42	10.44	10.38	10.53	10.45	10.75
	D_b^*	D_b															
Th	5.30	5.26	5.75	5.77	5.77	5.78	5.97	6.10	5.98	6.11	6.12	6.39	6.41	6.48	6.57	6.50	6.94

TABLE VIII. (*Continued.*)

	1^3S_1	1^1S_0	$^3P_0$	$^1P_1$	$^3P_1$	$^3P_2$	2^1S_0	$^3D_1$	2^3S_1	$^1D_2$	$^3D_3$	$^3F_2$	$^3F_4$	3^1S_0	2^3D_1	3^3S_1	4^3S_1
	F_b^*	F_b															
Th	5.37	5.31	5.77	5.80	5.80	5.82	5.96	6.09	5.99	6.11	6.12	6.35	6.37	6.41	6.50	6.43	6.82
	G^*	G															
Th	6.32	6.15	6.70	6.77	6.75	6.78	6.84	7.02	6.91	7.04	7.05	7.25	7.27	7.25	7.37	7.30	7.63
	T^*	T															
Th	27.44	−0.37	0.62	0.66	0.65	0.67	0.65	0.93	0.74	0.94	0.94	1.14	1.14	1.05	1.23	1.11	1.39

depend on meson masses or meson sizes according to the idea of asymptotic freedom. We decide to use the rms r_V of the $1\ ^3S_1$ vector meson of a family as the scaling parameter, since it has a smoother behavior than the meson mass. The $u\bar{u}$ and $c\bar{c}$ potential strengths then give us the following numerical expression based on the usual logarithmic scaling behavior[18]:

$$\alpha_s(V) = 1.4/[1 + 1.295 \ln(r_\rho/r_V)] . \quad \text{(A8)}$$

The strength k of the linear confinement potential turns out also to be different. In scaling, we use the numerical expression

$$k(V) = 0.0795[1 + 0.7115 \ln(r_\rho/r_V)] \text{ GeV}^2 . \quad \text{(A9)}$$

It is somewhat unfortunate that k is not a universal constant, as suggested by certain theoretical prejudices. Our "unusual" result should not be taken too literally, however, since we are describing relativistic systems such as light mesons in nonrelativistic terms.

If Eq. (A9) is used to generate values of k for NR potentials of other meson families, the calculated masses of the lightest vector mesons agree quite well (to within 30–50 MeV) with observed masses using the same additive constant b everywhere. Even better results in absolute masses are obtained if we interpolate not k, but the equivalent potential parameter

$$\omega = (4k^2/\mu)^{1/3} \quad \text{(A10)}$$

by using the empirical expression obtained from the independent $u\bar{u}$ and $c\bar{c}$ potentials

$$\omega(V) = 0.75/[1 + 0.4314 \ln(r_\rho/r_V)] \text{ GeV} . \quad \text{(A11)}$$

The results reported here are based on this equation.

We next note that if the meson radius controls the potential strengths, it is plausible that it also controls the cutoff parameter r_0. We use the simple power dependence

$$r_0(V) = \left(\frac{r_V}{r_\rho}\right)^{2.06} 1.05 \text{ fm} , \quad \text{(A12)}$$

where the numerical constants are also obtained from the $u\bar{u}$ and $c\bar{c}$ potentials. The same additive constant, $b = -0.08$ GeV, is used in all the other meson potentials.

Only two other quark masses, m_s and m_b, remain to be chosen. They are obtained by fitting the masses of $\phi(1.02)$ and $\Upsilon(9.46)$. The meson potentials are now completely defined. Their potential parameters are shown explicitly in Table VII. We note in summary that these potentials contain a total of thirteen adjustable parameters: four masses, two sets of potential strengths (α_s, k), two sets of cutoff parameters (r_0, a_0), and one ad-

ditive constant b.

Meson masses calculated from these NR potentials are shown in Table VIII, and compared with observed masses from Refs. 5, 20, 26, and 27. The general trend of the ≃45 meson masses is reproduced surprisingly well, given the relative simplicity of the model used. The following features are particularly noteworth: (1) All mesons are covered by our simple scaling formulas for potential parameters. Since the lighter mesons are certainly relativistic systems, it is clear that all relativistic effects have been absorbed into the potential parameters, leaving only a nonrelativistic caricature of the real dynamics. This is of course unsatisfactory, but one can also argue that from a certain limited perspective, this might well be a blessing in disguise. For example, this NR potential can readily be used in NR models of the properties of other hadrons. By virtue of the fitting procedure, there is some assurance that many of the calculated properties may be quite close to the actual values. As a consequence, some insight can be gained concerning certain hadron properties which are insensitive to the defects of the model. We have already mentioned some very reasonable results obtained by Rondinone and Wong[23] for the masses and sizes of certain baryons using the NR meson potentials obtained here. (2) There is some success in reproducing the spin dependence of meson masses with simple modifications of the short-range singular behavior of the Breit-Fermi interaction. The success is particularly noteworthy for the K^* and ψ/J families where the situation is most clearcut both experimentally and theoretically.

A number of problems can also be seen in Table VIII. (1) The model value of 0.24 GeV for the π/η mass is close to neither π nor η, but rather to their isospin-weighted center of mass at 0.24 GeV. (2) The $c\bar{c}$ potential reported here was obtained some time ago with 2.83 GeV as an input mass for η_c. It is clear now that $X(2.83)$ is not η_c, that there may not be an $X(2.83)$ at all, and that the real η_c is much closer to ψ/J, so that its contribution to the decay width of ψ/J is quite small, thus accounting for its relative invisibility. Since our hyperfine mass splittings look quite good for the K^* and D^* families, we decide to keep this old $c\bar{c}$ potential, and consider the model value of η_c as another bad $I=0$ pseudoscalar mass. This leads to a simple picture that all model $I=0$ pseudoscalars are too light (by the same 0.3 GeV in both η and η'), the model $I=1$ pseudoscalar π is too heavy, while model $I=\frac{1}{2}$ pseudoscalars are only a little too heavy. (3) The model $^3P_1$ state of the ω family is about 0.1 GeV lighter than the mass of the $D(1.28)$ meson. (4) The model $^1P_1$ and $^1D_2$ states are lower than the masses of the B, A_3, and Q_A mesons. We believe that the last difficulty is related ultimately to our neglect of the Darwin term in Eq. (A2). All these limitations should be borne in mind in applications using this NR potential model.

The scaling formulas Eqs. (A7), (A8), and (A11) can also be used for the mesons $b\bar{u}$, $b\bar{s}$, and $b\bar{c}$, which we shall call the D_b^*, F_b^*, and G^* families of mesons. The calculated potential parameters are shown in Table VII. Table VIII gives the meson masses for these mesons if the b quark is a color triplet. These mesons are of considerable theoretical interest because none should be seen if b is the color-sextet quark predicted in the SO(8) extended supergravity theory.[28]

Finally we show in Table VII the potential parameters for the $T^*=t\bar{t}$ family of mesons containing the t quark. Its mass is taken to be 14 GeV, as estimated by Harari, Haut, and Weyers[29] in their "generation-mixing" model of quark masses and Cabibbo angles. The resulting T^* meson mass spectrum is given in Table VIII.

APPENDIX B: ELECTROMAGNETIC RADIATION OPERATORS

The electromagnetic multipole radiation operators used in this paper are the nonrelativistic operators of Brennan and Sachs[30]:

$$M_{\sigma\lambda\mu}(k)=\frac{(2\lambda+1)!!}{\lambda+1}\frac{1}{k^\lambda}\sum_i e_i(f_{\sigma\lambda})_i Y^*_{\lambda\mu}(\hat{r}_i)\,, \quad \text{(B1)}$$

where σ denotes the type (E or M) of photon which has total spin λ, projection μ, and energy k. The sum i is over the single particles (i.e., quarks) in the system, for each of which

$$f_{E\lambda}=\left(\frac{\partial}{\partial r}rj_\lambda\right)-\frac{k}{2m}\left(3j_\lambda+r\frac{\partial j_\lambda}{\partial r}+2j_\lambda r\frac{\partial}{\partial r}\right)+\frac{k}{2m}\mu\vec{\sigma}\cdot\vec{l}j_\lambda\,, \quad \text{(B2)}$$

$$f_{M\lambda}=\frac{1}{2m}\left[2\vec{l}\cdot\vec{\nabla}j_\lambda-\mu\vec{\sigma}\cdot\vec{r}k^2j_\lambda+\vec{\nabla}\left(\frac{\partial}{\partial r}rj_\lambda\right)\right]. \quad \text{(B3)}$$

Except for the photon energy k and photon spin λ, all variables in these equations are single-particle variables, while $j_\lambda=j_\lambda(kr)$ is a spherical Bessel function.

The calculated results for the $E1$ and $M1$ widths for γ transitions between different charmonium states with masses in GeV shown explicitly inside brackets are given in Table IX. The three charmonium potentials used are potential A from Ref. 9, potential B from Ref. 1, and potential C from Appendix A. These results give indications of the model dependence expected in different γ widths.

TABLE IX. The widths in keV of $E1$ and $M1$ γ transitions between different charmonium states with masses (in GeV) shown inside brackets.

Potential	A	B	C
$E1$ transitions			
2^3S_1 (3.69) $\to {}^3P_2$ (3.55)	26	23	36
$\to {}^3P_2$ (3.59)	11	9	15
$\to {}^3P_1$ (3.51)	31	28	33
$\to {}^3P_1$ (3.45)	61	57	65
$\to {}^3P_0$ (3.41)	25	24	14
$\to {}^3P_0$ (2.83)	202	82	280
${}^3P_2$ (3.55) $\to {}^3S_1$ (3.10)	350	290	230
${}^3P_2$ (3.59) $\to$	400	340	260
${}^3P_1$ (3.51) $\to$	340	280	270
${}^3P_1$ (3.45) $\to$	230	190	180
${}^3P_0$ (3.41) $\to$	190	150	170
${}^3S_1$ (3.10) $\to {}^3P_0$ (2.83)	53	43	42
$M1$ transitions			
2^3S_1 (3.69) $\to 2^1S_0$ (3.59)	1.5	1.4	1.4
$\to 2^1S_0$ (3.45)	24	22	22
$\to {}^1S_0$ (2.83)	6.8	5.8	42
2^1S_0 (3.59) $\to {}^3S_1$ (3.10)	1.4	1.0	81
2^1S_0 (3.45) $\to$	0.2	0.14	26
${}^3S_1$ (3.10) $\to {}^1S_0$ (2.83)	34	31	33
2^3S_1 (3.69) $\to {}^1D_2$ (3.59)	2.4×10^{-5}	1.6×10^{-5}	3×10^{-5}
$\to {}^1D_2$ (3.45)	1.3×10^{-2}	9×10^{-3}	1.7×10^{-2}
${}^3D_1$ (3.69) $\to {}^1D_2$ (3.59)	0.63	0.59	0.7
$\to {}^1D_2$ (3.45)	10	9.5	12
${}^1D_2$ (3.59) $\to {}^3S_1$ (3.10)	0.21	0.13	0.16
$\to {}^3D_1$ (3.10)	170	150	190
${}^1D_2$ (3.45) $\to {}^3S_1$ (3.10)	0.022	0.014	0.017
$\to {}^3D_1$ (3.10)	54	50	61

Finally, we should mention that the D-state probabilities of the charmonium ${}^3S_1$ states as calculated for potential C are 0.10% for $\psi(3.10)$ and 0.06% for $\psi'(3.69)$.

APPENDIX C: MIXING MATRIX ELEMENT FOR $c\bar{c}g \leftrightarrow c\bar{c}q\bar{q}$

The $g \to q\bar{q}$ vertex in the mixing matrix element for $c\bar{c}g \to c\bar{c}q\bar{q}$ is

$$H(g\to q\bar{q}) = \vec{j}\cdot\vec{A}_g = -i\bar{u}^{(s')}(\vec{p}')\gamma v^{(s)}(\vec{p})\cdot\vec{A}_g$$
$$= \left[\left(\frac{E+m}{2E}\right)\left(\frac{E'+m}{2E'}\right)\right]^{1/2}(-)^{1/2+s}$$
$$\times\chi^{(s')\dagger}\left[\vec{\sigma} - \frac{(\vec{\sigma}\cdot\vec{p}')\vec{\sigma}(\vec{\sigma}\cdot\vec{p})}{(E+m)(E'+m)}\right]\chi^{(s)}\cdot\vec{A}, \quad \text{(C1)}$$

in the notation of Ref. 31. (The quark momenta are $\vec{p}$ and $\vec{p}'$.) To calculate its matrix element

$$h(g\to q\bar{q}) \equiv \langle {}^3S_1{}^8(q\bar{q})\,|\,H(g\to q\bar{q})\,|\,{}^3s_1{}^8(g)\rangle, \quad \text{(C2)}$$

we approximate the center-of-mass wave function of the $q\bar{q}$ pair by the gluon wave function ϕ_g of $c\bar{c}g$ shown in Eq. (3.2), while the relative $q\bar{q}$ wave function is taken to be the relative $c\bar{c}$ wave function $2^{-3/2}\,\phi_{c\bar{c}}=R_{c\bar{c}}/\sqrt{4\pi}$ since $q\bar{q}$ is in the same bag as $c\bar{c}$. This approximation is very rough, but appears to be consistent with the many shortcomings of the model. For the nonrelativistic $\vec{\sigma}\cdot\vec{A}_g$ term, we readily obtain the result for $m_q \ll E_q$ of

$$h_{\rm NR}(g\to q\bar{q}) \simeq g\left(\tfrac{2}{3}\right)^{1/2}\frac{\pi}{2}R_{c\bar{c}}(0)\int_0^\infty dk\,k^{3/2}\vec{\phi}_g{}^2(k) = A\mu^{3/2}\lambda^{-1/2}, \quad \text{(C.3)}$$

where

$$A=g\left(\tfrac{2}{3}\right)^{1/2}\frac{\pi}{8}\int_0^\infty dx\,x^{3/2}\left[\frac{2}{\pi^2\left(\frac{1}{4}+x^2\right)^4}\right]=0.16\,, \qquad x=k/\lambda\,. \quad \text{(C4)}$$

The second term of Eq. (C1) turns out to be proportional to $\vec{p}\cdot\vec{p}'$. This averages to zero for two S-wave quarks q and $\bar{q}$. Hence $h=h_{\rm NR}$.

[1] K. Gottfried, in *Proceedings of the 1977 International Symposium on Lepton and Photon Interactions at High Energies*, edited by F. Gutbrod (DESY, Hamburg, Germany, 1977), p. 667.

[2] C. J. Biddick *et al.*, Phys. Rev. Lett. 38, 1324 (1977).

[3] W. Bartel *et al.*, Phys. Lett. 79B, 492 (1978).

[4] W. Braunschweig *et al.*, Phys. Lett. 67B, 243 (1977); 67B, 249 (1977); S. Yamada, in *Proceedings of the 1977 International Symposium on Lepton and Photon Interactions at High Energies* (Ref. 1), p. 69.

[5] Particle Data Group, Phys. Lett. 75B, 1 (1978).

[6] E. Bloom, preliminary results of the Crystal Ball Experiment, presented at the Fermilab Conference, 1979 (unpublished) and private communications. We would like to thank Dr. Bloom for permission to quote these preliminary results.

[7] F. Bolos *et al.*, as reported in the APS meeting at Washington, 1979, in a post-deadline paper (unpublished).

[8] G. S. Abrams *et al.*, Report No. SLAC-PUB-2350-LBL-9320, 1979, paper presented at the International Conference on High Energy Physics, Geneva, 1979 (unpublished).

[9] E. Eichten *et al.*, Phys. Rev. Lett. 34, 369 (1975).

[10] D. Horn and J. Mandula, Phys. Rev. D 17, 898 (1978).

[11] R. L. Jaffe, Phys. Rev. D 15, 267 (1977); 15, 281 (1977); minor errors in the recoupled wave functions of the $J=0$ mesons have been corrected by C. W. Wong and K. F. Liu, Phys. Rev. D (to be published).

[12] A. De Rújula and R. L. Jaffe, in *Experimental Meson Spectroscopy 1977*, proceedings of the Fifth International Conference, edited by E. Von Goeler and R. Weinstein (Northeastern University, Boston, 1977), p. 83.

[13] See, for example, D. Robson, Nucl. Phys. B130, 328 (1977).

[14] H. J. Lipkin, H. R. Rubinstein, and N. Isgur, Phys. Lett. 78B, 295 (1978).

[15] R. L. Jaffe and K. Johnson, Phys. Lett. 60B, 201 (1976).

[16] E. B. Dally *et al.*, Phys. Rev. Lett. 39, 1176 (1977).

[17] T. Appelquist and H. D. Politzer, Phys. Rev. Lett. 34, 43 (1975).

[18] D. J. Gross and F. Wilczek, Phys. Rev. Lett. 30, 1343 (1973); H. D. Politzer, *ibid.* 30, 1346 (1973).

[19] S. O. Holmgren and M. R. Pennington, Phys. Lett. 77B, 304 (1978).

[20] D. W. G. S. Leith, in *Experimental Meson Spectroscopy 1977* (Ref. 12), p. 207.

[21] G. K. Greenhut, Bull. Am. Phys. Soc. 24, 559 (1979).

[22] See, for example, E. Eichten, in *New Results in High Energy Physics—1978*, proceedings of the Third International Conference at Vanderbilt University on High Energy Physics, edited by R. S. Panvini and S. E. Csorna (AIP, New York, 1978), p. 252.

[23] J. F. Rondinone, Ph. D. thesis, UCLA, 1978 (unpublished); J. F. Rondinone and C. W. Wong, 1978 (unpublished).

[24] F. Borkowski *et al.*, Nucl. Phys. A222, 269 (1974).

[25] K. F. Liu and C. W. Wong, Phys. Rev. D 17, 2350 (1978); Phys. Lett. 73B, 223 (1978).

[26] R. Brandelik *et al.*, Phys. Lett. 76B, 361 (1978).

[27] K. Ueno *et al.*, Phys. Rev. Lett. 42, 486 (1979).

[28] D. Z. Freedman, *in Particles and Fields—1977*, proceedings of the meeting of the Division of Particles and Fields of the APS, Argonne, edited by P. A. Schreiner *et al.* (AIP, New York, 1978), p. 65.

[29] H. Harari, H. Haut, and J. Weyers, Phys. Lett. 78B, 459 (1978).

[30] J. G. Brennan and R. G. Sachs, Phys. Rev. 88, 824 (1952).

[31] J. J. Sakurai, *Advanced Quantum Mechanics* (Addison-Wesley, Reading, Mass., 1967), Chap. 3.